
Figures and figure supplements

Regulation of pulmonary surfactant by the adhesion GPCR GPR116/ADGRF5 requires a tethered agonist-mediated activation mechanism

James P Bridges *et al*

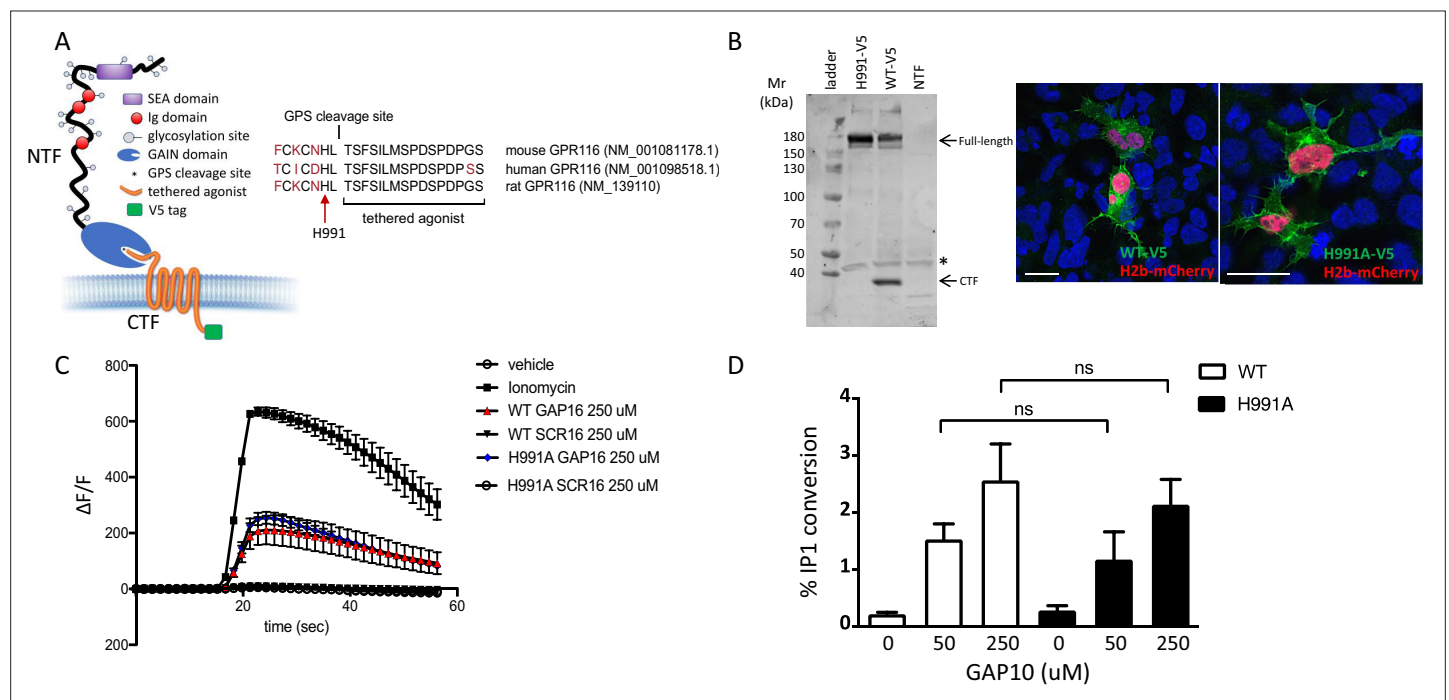


Figure 1. Generation and validation of a non-cleavable GPR116 mutant H991A. **(A)** Schematic representation of the H991A mutation in GPR116, details of the sequence at the protein level and gene references. **(B)** Transient expression of V5-tagged H991A in HEK293 cells shows no cleavage at the GPS site by Western blot compared to the wild-type receptor; membrane localization by V5 immunocytochemistry shows similar localization of WT-V5 and H991A-V5. NTF, non-transfected control. Asterisk denotes non-specific band. Scale bars = 25 μ m. See also **Figure 1—source data 1**. **(C, D)** Functional characterization of mouse GPR116 H991A in calcium transient assays **(C)** and in IP1 accumulation assays **(D)**, using GAP16, GAP10, or scrambled peptide (SCR16) as the stimulus ($n = 3$ independent experiments performed with $n = 1$ technical replicate for **C** and $n = 2$ technical replicates per group for **D**). Data are expressed as mean \pm SD (one-way ANOVA for **C** and **D**). ns, not significant.

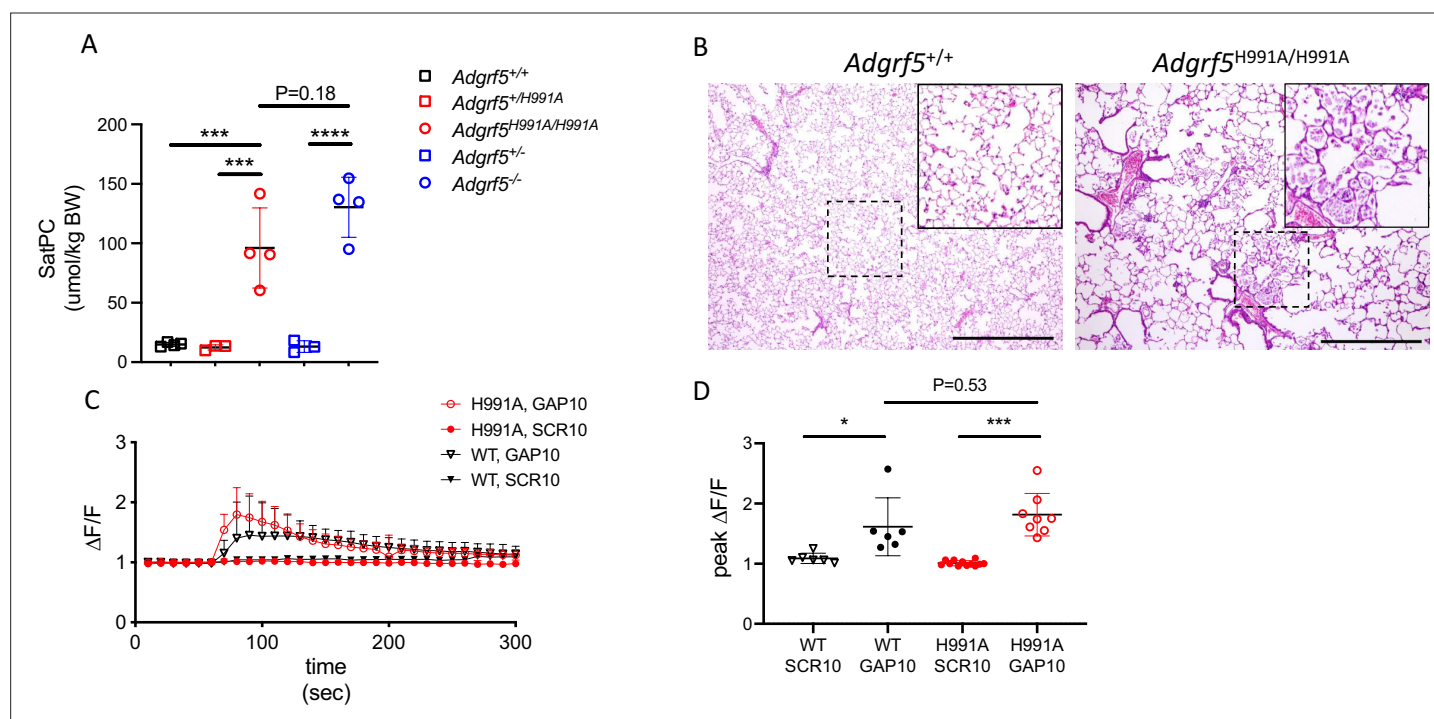


Figure 2. Cleavage at the GPS site is required for GPR116 function in vivo. **(A)** Content of saturated phosphatidylcholine (SatPC) in the bronchoalveolar lavage fluid (BALF) of 8-week-old wild-type (*GPR116*^{+/+}), *GPR116*^{+/H991A}, *GPR116*^{H991A/H991A} (line 2552), *GPR116*^{+/-}, and *GPR116*^{-/-} mice (*n* = 3–4 mice per group). Data are expressed as mean ± SD (one-way ANOVA). ****p* < 0.001, *****p* < 0.0001. **(B)** Representative histology of 4.5-month-old wild-type and homozygous H991A knock-in mice. Note accumulation of pulmonary surfactant (inset) and alveolar simplification in H991A knock-in mice compared to wild-type control. Scale bars = 500 μm. **(C)** GAP10-induced calcium transients in primary AT2 cells of *GPR116*^{+/+} and *GPR116*^{H991A/H991A} mice (*n* = 3–4 independent experiments, *n* = 3 biological replicates per group). Data are expressed as mean ± SD. **(D)** Peak calcium responses in primary *GPR116*^{+/+} (WT) and *GPR116*^{H991A/H991A} AT2 cells treated with SCR10 or GAP10 (*n* = 3 independent experiments, with *n* = 2–3 technical replicates per group). Data are expressed as mean ± SD (one-way ANOVA). **p* < 0.01, ****p* < 0.001.

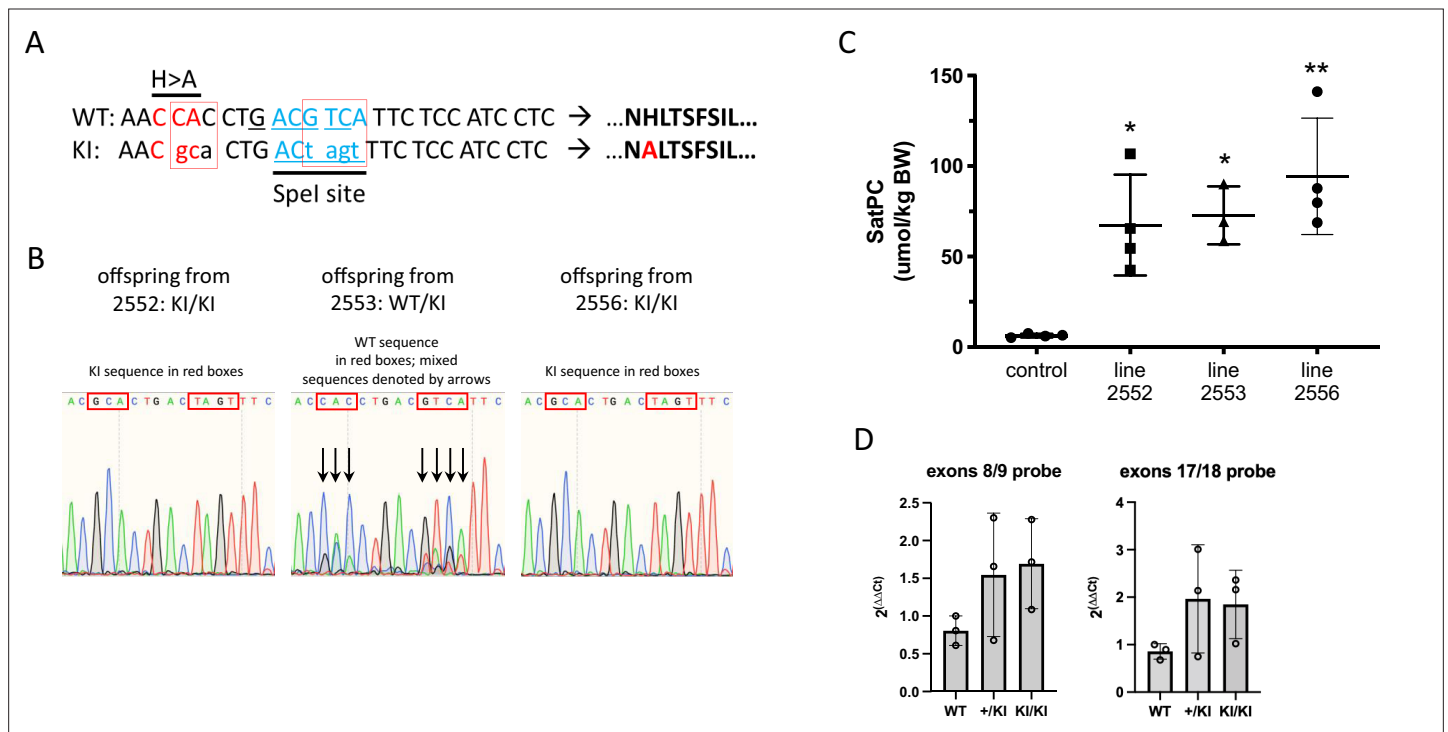


Figure 2—figure supplement 1. Schematic of H991A point mutation introduced into the *Adgrf5* locus via CRISPR/Cas9 gene editing. **(A)** Red boxes denote introduced base pair changes in the *Adgrf5* locus. Spel restriction enzyme recognition site was introduced for screening purposes without altering amino acid sequence at this position. **(B)** Representative sequencing traces of genomic DNA from two homozygous (2552 and 2556) and one heterozygous H991A line (2553). Line 2553 was bred to homozygosity for experiments. **(C)** Content of saturated phosphatidylcholine (SatPC) in the bronchoalveolar lavage fluid (BALF) of 4-week-old wild-type control and H991A homozygous knock-in mice ($n = 3\text{--}4$ mice per group). **(D)** qPCR analysis of GPR116 expression in isolated AT2 cells from WT, line 2552 H991A KI heterozygous mice (+/KI) and line 2552 H991A homozygous mice (KI/KI). Each data point represents a cell preparation from an individual animal. Data are expressed as mean \pm SD (one-way ANOVA). ** $p < 0.005$, * $p < 0.05$.

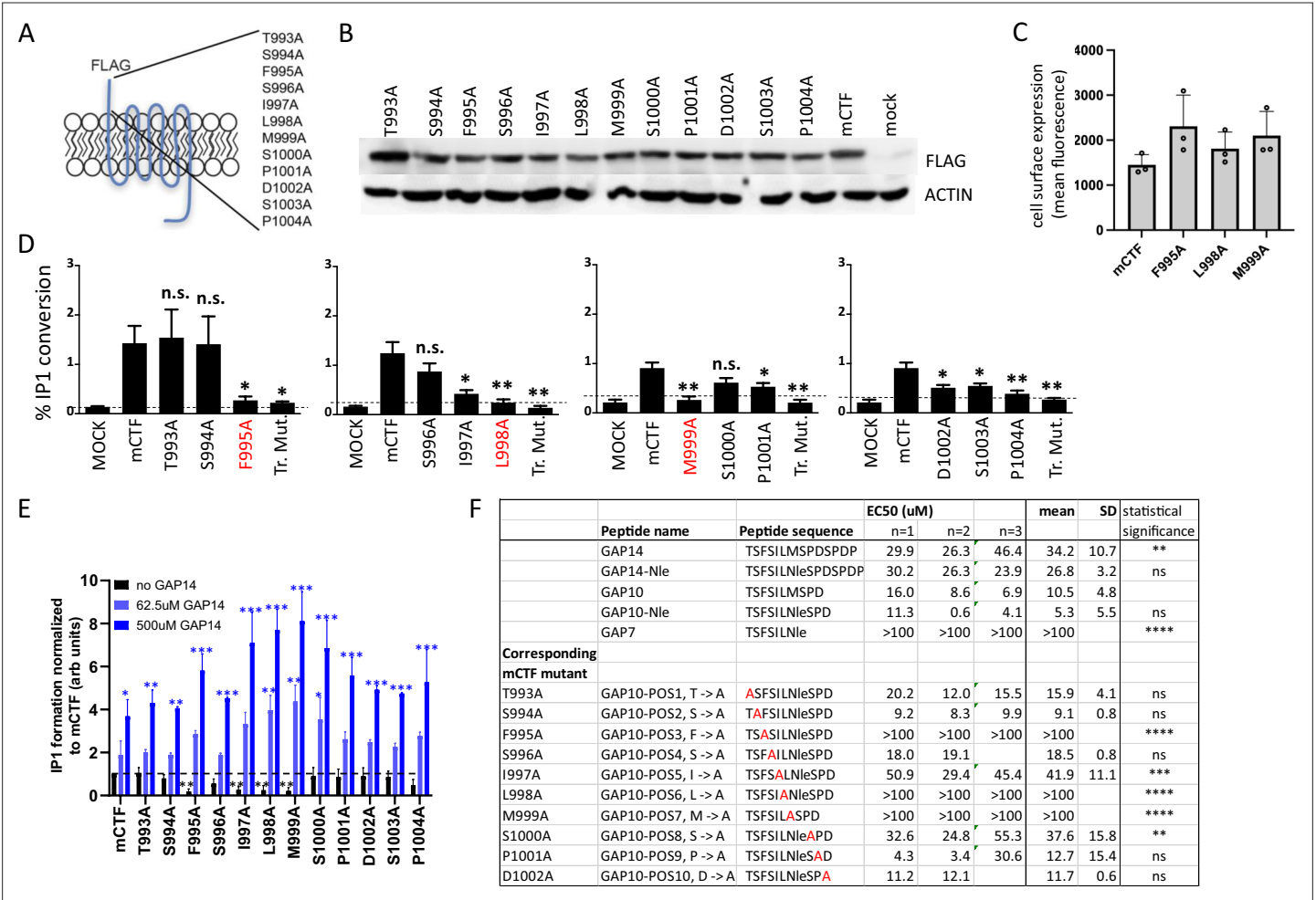


Figure 3. Identification of amino acids in the tethered agonist essential for GPR116 activity. **(A)** Design of the 12 mGPR116 CTF (mCTF) ECD mutants. Alanine scan of individual residues in the N-terminal sequence. **(B)** Expression of the mCTF ECD mutants transiently expressed in HEK293 cells. Constructs were detected by Western blot of whole-cell lysates using an anti-FLAG antibody. Molecular weight of FLAG ~43kDa; molecular weight of actin ~42kDa. See also **Figure 3—source data 1 and 2**. **(C)** Quantitation of cell surface expression of mCTF ECD mutants by anti-FLAG antibody staining and flow cytometry of non-permeabilized cells. **(D)** Signaling of the mGPR116 CTF ECD mutants. Constructs of the ECD alanine scan and corresponding triple mutants were transiently expressed in HEK293 cells and basal activity was measured as % IP1 conversion ($n = 4\text{--}5$ independent experiments, with $n = 2$ technical replicates per group). Dashed line indicates background activity as reference. Data are expressed as mean \pm SD. $**p < 0.01$, $*p < 0.05$. The three single-point mutants with the most potent inhibitory effect are highlighted in red. Tr. Mut., triple mutant. **(E)** Exogenous GAP14 treatment rescues mCTF ECD mutants with inactive tethered agonist and super-activates constructs exhibiting basal activity. Constructs were transiently expressed in HEK293 cells and stimulated with GAP14. IP1 accumulation was measured in $n = 2\text{--}3$ independent experiments with $n = 2\text{--}4$ replicates to evaluate basal and GAP14-induced activity of the receptor, respectively. Data are expressed as mean \pm SD. Basal activity of mCTF (dashed line) was used as the reference. Basal or GAP14-induced activities significantly different from mCTF baseline are marked with black or blue stars, respectively. $*p < 0.05$, $**p < 0.01$, $***p < 0.001$. **(F)** Activation of full-length mGPR116 in stable expressing cells (HEK293 clone 3C) with exogenous GAP10 peptides that were sequentially mutated to alanine at each position. Receptor activation was measured via calcium transient assays, in $n = 2\text{--}3$ independent experiments, with $n = 4$ technical replicates per group. Quadruplicate means of each experiment and final mean \pm SD are detailed. $**p < 0.01$, $***p < 0.001$, $****p < 0.0001$. See also **Figure 3—source data 3**.

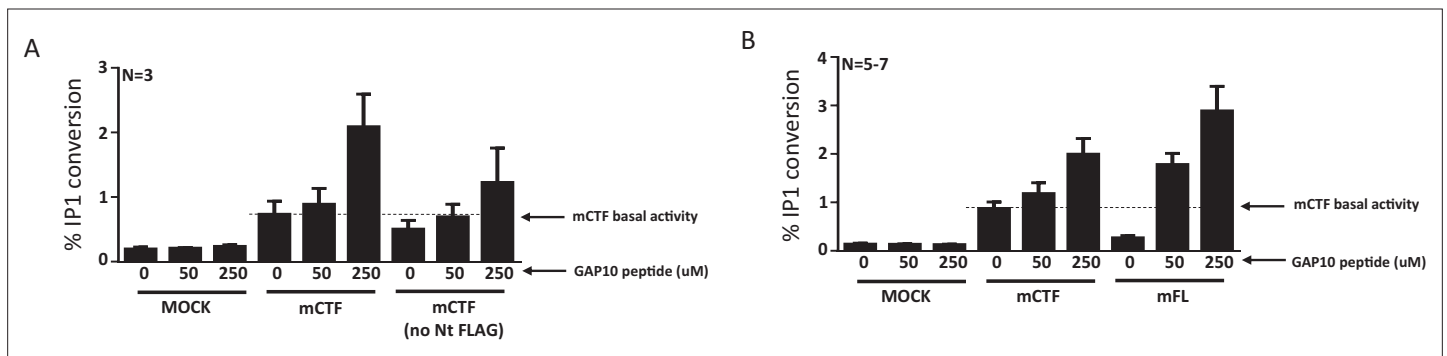


Figure 3—figure supplement 1. Super-activation of mGPR116 C-terminal fragment (CTF) constructs with basal activity. **(A)** The N-terminal FLAG tag in the mCTF constructs does not affect the activation by GAP10. Tagged and untagged mCTF were transiently expressed in HEK293 cells and GAP10-induced IP1 conversion was measured. Dotted line indicates mCTF basal activity; $n = 3$ independent experiments, with $n = 2$ technical replicates per group. Data are expressed as mean \pm SD. **(B)** The mCTF construct, expressed transiently in HEK293 cells, shows basal activity and can be super-activated to levels approximating that of the full-length receptor (mFL) upon addition of GAP10. Receptor signaling is measured in the IP1 conversion assay; $n = 5-7$ independent experiments with $n = 3$ technical replicates per group. Data are expressed as mean \pm SD.

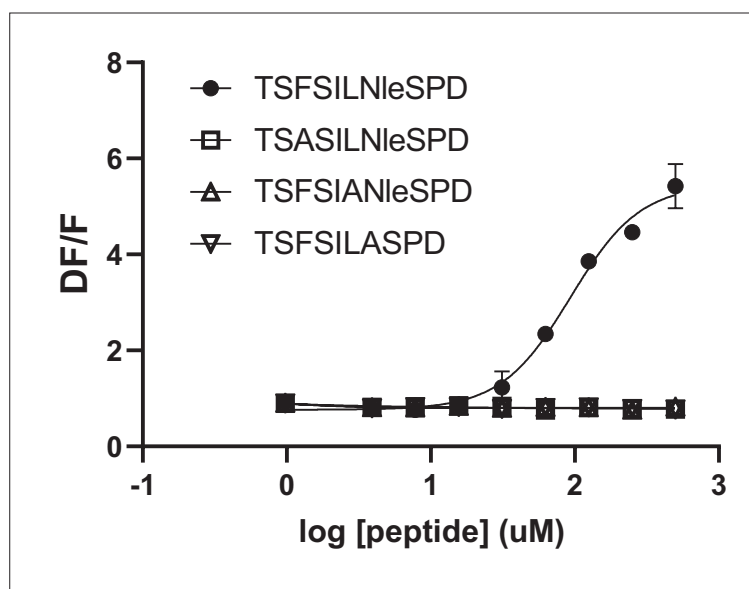


Figure 3—figure supplement 2. Alanine mutation of key amino acids in GAP10 inactivates the peptide for human GPR116 full-length stimulation. Full-length hGPR116 (HEK293 clone A6) stimulated with GAP10 and peptide variants corresponding to alanine changes identified in mGPR116 as being critical for the activation by the tethered agonist ($n = 5\text{--}7$ independent experiments, with $n = 2$ technical replicates per group). Data are expressed as mean \pm SD. See **Supplementary file 2** for EC50 and statistical details.

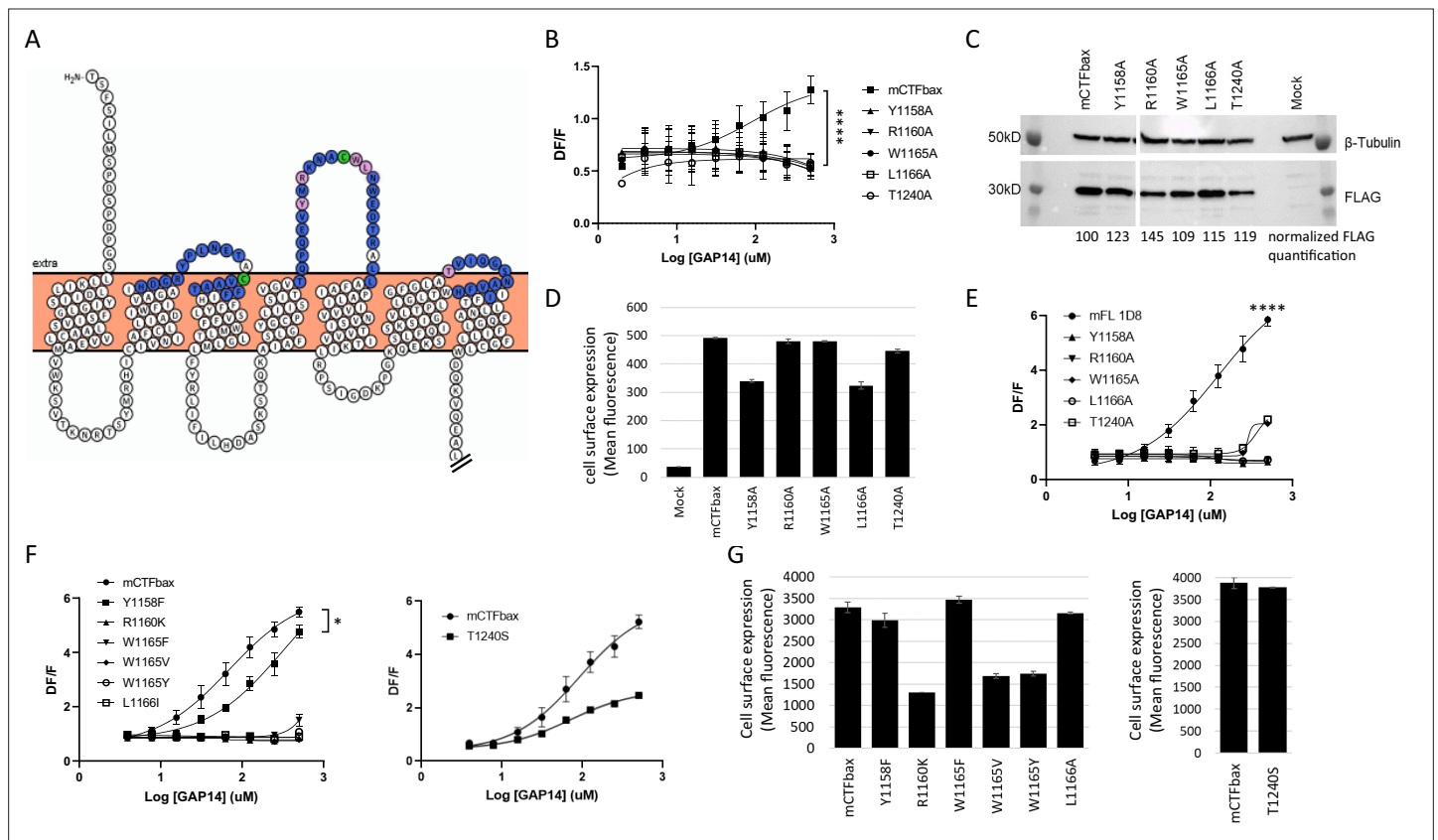


Figure 4. Identification of key extracellular loop (ECL) amino acids involved in GPR116 activation by the tethered agonist.

(A) Snake plot model of mouse GPR116 C-terminal fragment (CTF). ECL residues individually mutated in the alanine scan of mouse GPR116 CTF constructs tested for functional activity are colored in blue or pink; the five residues shown in pink were identified as strongly modulating receptor activity. The two cysteine residues forming the disulfide bridge are shown in green. The Ct tail was truncated for visualization purposes as indicated by double hash lines. (B) Alanine scan of ECLs in mCTFbax, a CTF construct without basal activity. Calcium transient assays were performed in transiently transfected HEK293 cells with exogenous GAP14 as the stimulus. mCTFbax mutants that were completely inactive following GAP14 stimulation are shown. Data are from $n = 3$ independent experiments, with $n = 4$ technical replicates per group. Data are expressed as mean \pm SD (**** $p < 0.0001$ for the reference construct vs. mutants). See **Figure 4—figure supplement 1A** for further alanine scan data, including mutants with no effect. See **Supplementary file 2** for potency and statistical details. (C, D) Expression of the mCTFbax mutants not activated by GAP14, in transiently transfected HEK293 cells. (C) Proteins were detected by Western blot using an anti-FLAG antibody. For quantification, levels of FLAG signal were normalized to tubulin expression and expressed as % of mCTFbax levels. See also **Figure 4—source data 1–3**. (D) Surface levels of receptor expression was measured by flow cytometry using an anti-FLAG antibody on non-permeabilized cells. Data are expressed as mean \pm SD from an experiment with duplicates. (E) GAP14-induced calcium transients of mFL mutants for five key ECL residues, stably expressed HEK293 cells, as compared to the WT mGPR116 1D8 clone. Data shown are from $n = 3$ independent experiments with $n = 4$ technical replicates per group. Data are expressed as mean \pm SD (**** $p < 0.0001$ for the reference construct vs. mutants). See **Supplementary file 2** for potency and statistical details. (F) Mutation of key ECL residues in the mCTFbax construct to amino acids with functional relevance. mCTFbax and mutants thereof were stably expressed in HEK293 cells and GAP14-induced calcium transients were measured. Data are from $n = 3$ independent experiments, with $n = 4$ technical replicates per group. Data are expressed as mean \pm SD (* $p < 0.05$). See **Supplementary file 2** for potency and statistical details. (G) Surface levels of receptor expression for mCTFbax mutants in HEK293 stable populations were measured by flow cytometry using an anti-FLAG antibody. Data are expressed as mean \pm SD from an experiment with duplicates.

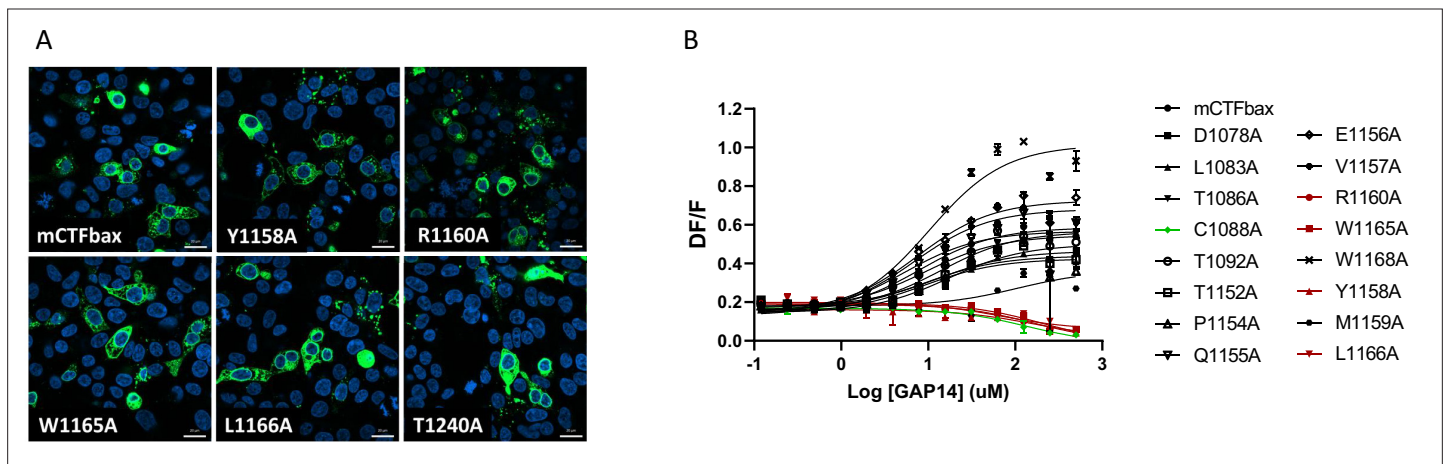


Figure 4—figure supplement 1. Alanine scan of GPR116 C-terminal fragment (CTF) extracellular loops (ECLs). **(A)** Expression of the mCTFbax mutants not activated by GAP14, in transiently transfected HEK293 cells; detection by V5 tag immunocytochemistry (scale bars = 20 μm). **(B)** Representative data from mutants with or without functional effect. Calcium transient assays were performed in transiently transfected HEK293 cells with exogenous GAP14 as the stimulus. mCTFbax mutants with varying effects of the mutation are shown. Mutants exhibiting no activity upon GAP14 stimulation and selected for further analysis are highlighted in red, and the construct with one of the cysteines from the disulfide bridge mutated to alanine is in green. Data are from n = 1 experiment, with n = 4 technical replicates per group. Data are expressed as mean ± SD.

	tethered peptide (993 - 1008)			
hGPR116 CTF	TSFSILMSPDSPDPSS			
mGPR116 CTF	TSFSILMSPDSPDPGS			
	TM1 (1009 - 1038)	ICL1 (1039 - 1054)	TM2 (1055 - 1080)	ECL1 (1081 - 1087)
hGPR116 CTF	LLGILLDIISYVGVGFSILSLAACLVVEAV	VWKSVTKNRTSYMRHT	CIVNIAASLLVANTWFIIVAAIQDNR	YILCKTA
mGPR116 CTF	LLKILLDIISYIGLGFSIVSLAACLVVEAM	VWKSVTKNRTSYMRHI	CIVNIAFCLLIADIWFIIVAGAIHDGR	YPLNETA
	TM3 (1088 - 1113)	ICL2 (1114 - 1130)	TM4 (1131 - 1152)	ECL2 (1153 - 1174)
hGPR116 CTF	CVAATFFIHFFYLSVFFWMLTLGLML	FYRLVFILHETSRSTQK	AIAFCLGYGCPLAISVITLGAT	QPREVYTRKNVCWLNWEDTKAL
mGPR116 CTF	CVAATFFIHFFYLSVFFWMLTLGLML	FYRLIFILHDASKSTQK	AIAFSLGYGCPLIISITVGVF	QPQEVYMRKNACWLNWEDTRAL
	TM5 (1175 - 1200)	ILC3 (1201 - 1209)	TM6 (1210 - 1239)	ECL3 (1240 - 1245)
hGPR116 CTF	LAFaipALiIvVvNIITITIVVITKIL	RPSIGDKPC	KQEKSSLFQISKSIGVLTPLLGLTWGFGLT	TVFPGT
mGPR116 CTF	LAFaipALiIvVvNVSITVVVITKIL	RPSIGDKPG	KQEKSSLFQISKSIGVLTPLLGLTWGFGLA	TVIQGS
	TM7 (1246 - 1271)	Ct tail (1272 - 1348)		
hGPR116 CTF	NLVFHIIIFAILNVFQGLFILLFGCLW	DLKVQEALLNKFSLSRWSSQHSKSTS	LGSTPVMSSPISRFRNNLFGKTGTYNVSTPE	ATSSSLENSSSASLLN
mGPR116 CTF	NAVFHIIIFTLNAFQGLFILLFGCLW	DQKVQEALLHKFSLSRWSSQHSKSTS	IGSTPVMSSPISRFRNNLFGKTGTYNVSTPE	TSSSLENSSSAYSLLN

Figure 4—figure supplement 2. Alignment of the human and mouse GPR116 C-terminal fragment (CTF) sequences. Residues that are not conserved between the two species are highlighted in red and bold.

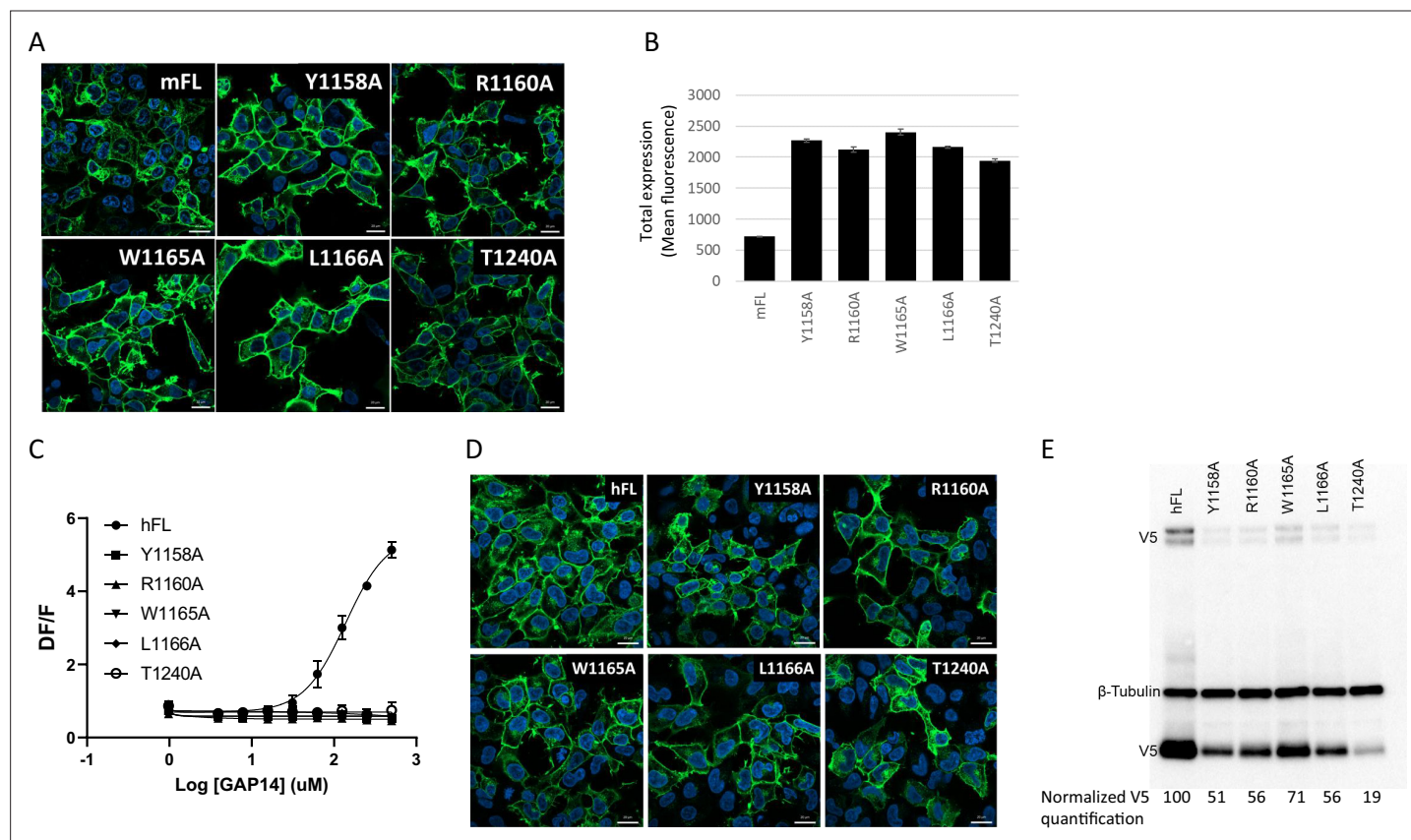


Figure 4—figure supplement 3. Mutation of the key extracellular loop (ECL) amino acids in mGPR116 full-length (mFL) WT (clone 1D8) and ECL mutants, as well as in human GPR116 full-length leads to inactive constructs. **(A)** Expression of the mGPR116 full-length (mFL) WT (clone 1D8) and ECL mutants assessed by V5 tag immunocytochemistry upon stable expression in HEK293 (scale bars = 20 um). **(B)** Expression of mFL ECL mutants stably expressed in HEK293 cells. Total expression levels were quantified in permeabilized cells by flow cytometry using an anti-V5 antibody. Data are expressed as mean \pm SD from an experiment with duplicates. **(C)** Activity of the full-length hGPR116 mutated for key ECL2/TM6 residues compared to the WT hGPR116 A6 clone (hFL). Mutants were stably expressed in HEK293 cells and GAP14-induced calcium transients were measured. Representative data of $n = 3$ independent experiments with $n = 4$ technical replicates per group. Data are expressed as mean \pm SD. See **Supplementary file 2** for potency and statistical details. **(D)** Expression of hFL WT (clone A6) and mutants was tested as HEK293 stable populations by V5 tag immunocytochemistry (scale bars = 20 um). **(E)** Expression of hFL WT (clone A6) and mutants in stably transfected HEK293 cells. Constructs were detected by Western blot using an anti-V5 antibody. The major band (~43 kDa) corresponds to the cleaved C-terminal fragment (CTF) and the minor bands at high molecular weight (~185 kDa) correspond to the full-length receptor. The levels of CTF V5 signal were quantified, normalized to tubulin expression (~50 kDa) and expressed as % of mCTFbax levels. See also **Figure 4—source data 5 and 6**.

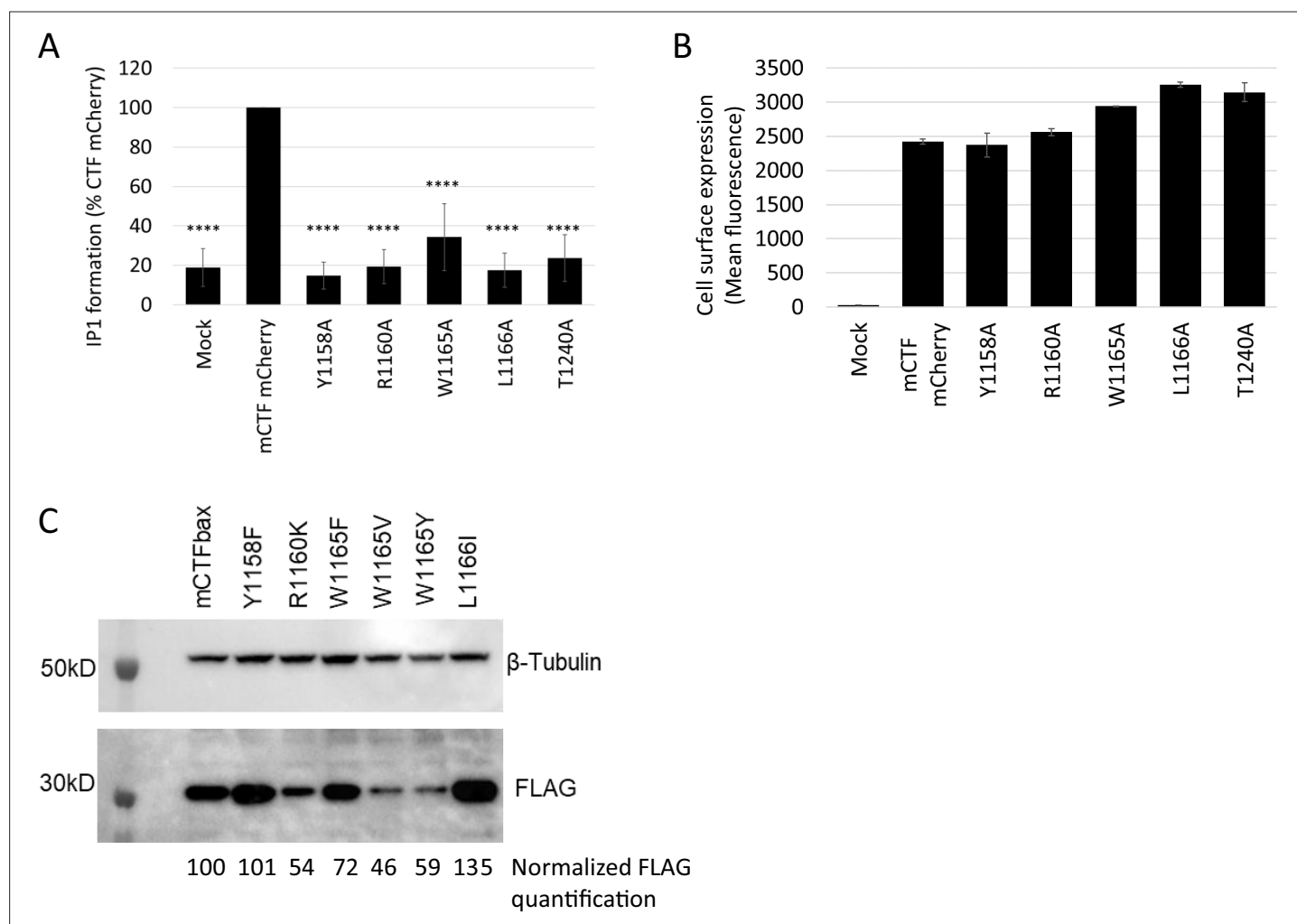


Figure 4—figure supplement 4. Alanine mutation of key extracellular loop (ECL) residues in mGPR116 C-terminal fragment (CTF) constructs with basal activity and non-conservative mutations in mCTFbax. **(A)** Basal activity of ECL mutants in the mCTF mCherry parent construct. ECL residues important for activation were mutated to alanine and IP1 formation was measured in transiently transfected HEK293 cells. Data, normalized to the parent construct, are expressed as mean \pm SD ($n=8$ independent experiments, with $n = ?$ (Marie?) technical replicates per group; **** $p<0.0001$). **(B)** mCTF mCherry constructs were transiently expressed in HEK293 cells, and expression was evaluated by flow cytometry analysis of the mCherry signal. Data are expressed as mean \pm SD from an experiment with duplicates. **(C)** Expression of mCTFbax mutants in HEK293 stable populations was analyzed by Western blot using the FLAG tag. For quantification, levels of FLAG signal were normalized to tubulin expression and expressed as % of mCTFbax levels. See also **Figure 4—source data 7–9**.

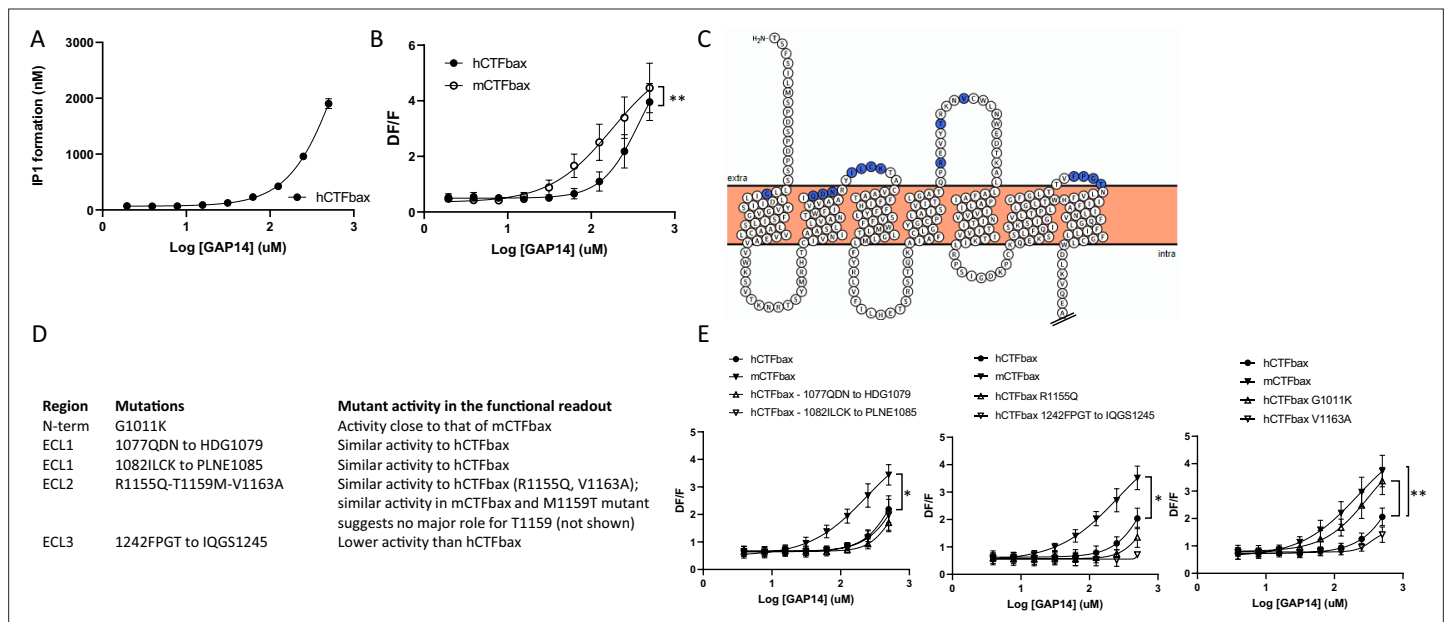
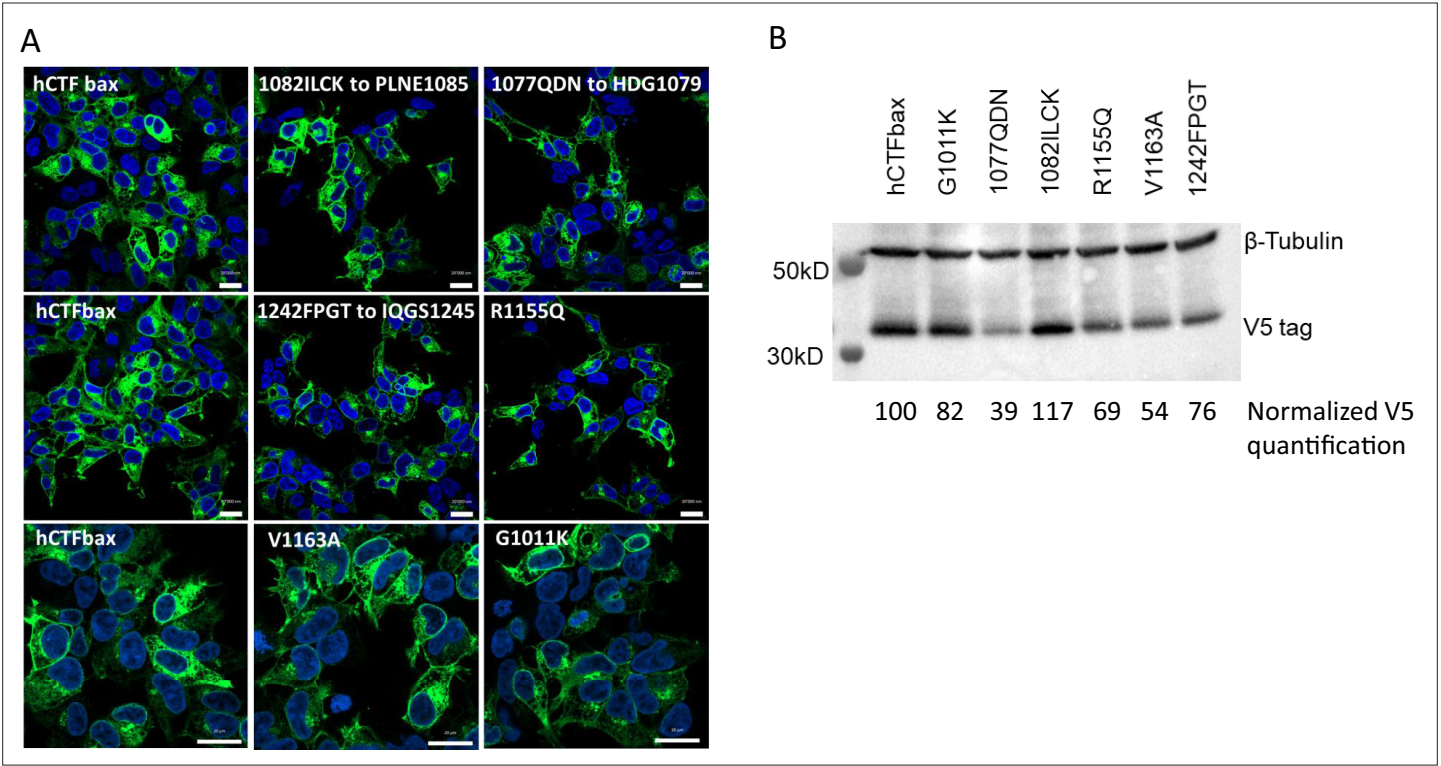


Figure 5. Evaluation of the role of extracellular loop (ECL) amino acids not conserved between human and mouse GPR116. **(A)** Characterization of hCTFbax, a C-terminal fragment (CTF) construct without basal activity and that can be activated by GAP14. The hCTF with deletion of the N-terminal six amino acids was stably expressed in HEK293 cells and stimulated with GAP14 in an IP1 accumulation assay ($n = 3$ independent experiments, with $n = 2$ technical replicates per group). Data are expressed as mean \pm SD. The basal level of IP1 formation in presence of LiCl is similar to that of parental HEK cells (inset). **(B)** Stable HEK293 populations for mCTFbax and hCTFbax were stimulated with GAP14 and analyzed for induction of calcium transients. Data from $n = 3$ independent experiments, with $n = 2$ technical replicates per group. Data are expressed as mean \pm SD (** $p < 0.01$). See **Supplementary file 2** for potency and statistical details. **(C)** Overview of the mouse-specific residues introduced in the hCTFbax construct. Snake plot of the human GPR116 CTF (including the full tethered agonist sequence); amino acids highlighted in blue, located towards to extracellular side, are not conserved between human and mouse GPR116. The corresponding mouse sequence was introduced in human GPR116. The Ct tail was truncated for visualization purposes as indicated by double hash lines. **(D)** Details of the residues exchanged in the hCTFbax with the corresponding mouse sequence. Each cluster of changes was tested for its signaling capacity and the functional assay outcome is described. **(E)** GAP14-induced calcium transients were not further increased in the mutants as compared to the reference construct hCTFbax with the exception of G1011K (right panel). Constructs were stably expressed in HEK293 cells and tested with $n = 2$ –4 technical replicates ($n = 4$ –5 independent experiments; data are expressed as mean \pm SD; * $p < 0.05$, ** $p < 0.01$). See **Supplementary file 2** for potency and statistical details.



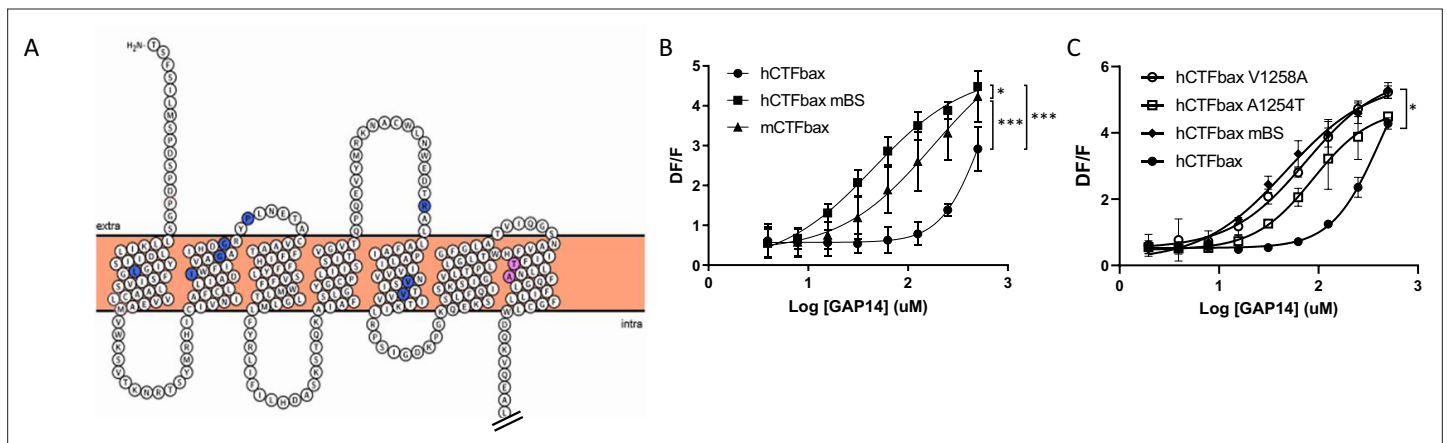
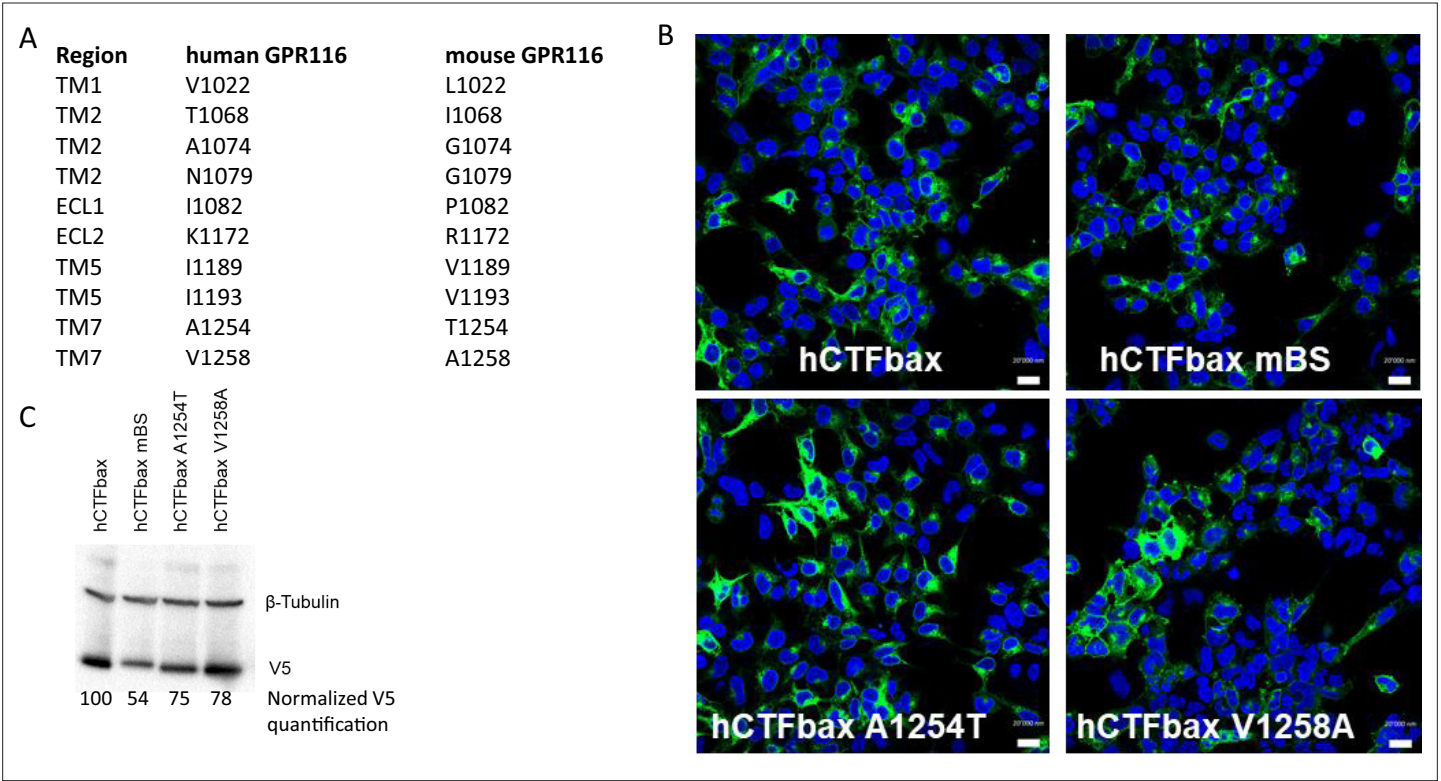


Figure 6. Engineering the predicted mouse GPR116 binding site (mBS) into human GPR116 leads to increased peptide activation. **(A)** Snake plot of the mouse GPR116 CTF highlighting mouse-specific amino acids in the putative binding site in blue and pink. Amino acids responsible for mGPR116-specific aspects of receptor activation are shown in pink. The Ct tail was truncated for visualization purposes as indicated by double hash lines. **(B)** Stable HEK293 populations for m/hCTFbax and hCTFbax mBS were stimulated with GAP14 and analyzed for the induction of calcium transients ($n = 3$ independent experiments, with $n = 2$ technical replicates per group; data are expressed as mean \pm SD; $*p < 0.05$, $***p < 0.001$). See **Supplementary file 2** for potency and statistical details. **(C)** Characterization of the key amino acids transmitting the effects of the mouse binding site sequence. hCTFbax single mutants were compared to hCTFbax and hCTFbax mBS in calcium transient assays. Stable HEK293 populations were stimulated with GAP14 ($n = 3$ independent experiments, with $n = 2$ duplicates per group; data are expressed as mean \pm SD; $*p < 0.05$ between hCTFbax and hCTFbax mBS). See **Supplementary file 2** for potency and statistical details.



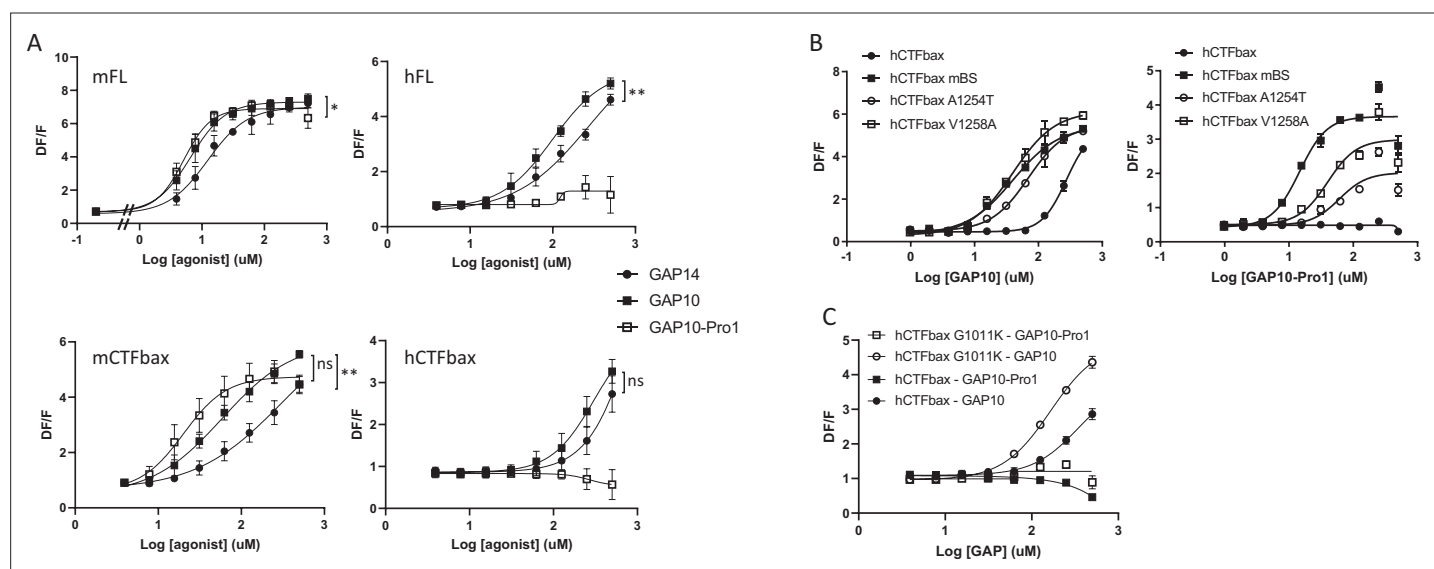


Figure 7. Characterization of a mouse-specific agonistic peptide. **(A)** GAP10-Pro1 only activates mouse GPR116. Full-length mouse and human GPR116 (mFL clone 3C and hFL clone A6, respectively), mCTFbax and hCTFbax, all stably expressed in HEK293 cells, were stimulated with GAP14, GAP10, and GAP10-Pro1. Calcium transients are measured as a signaling readout in $n = 3$ –4 independent experiments, with $n = 2$ –4 technical replicates per group. Data are expressed as mean \pm SD (* $p < 0.05$, ** $p < 0.01$). See **Supplementary file 2** for potency and statistical details. **(B)** Identification of the key amino acids mediating the mouse-specific effects in the mouse binding site. The hCTFbax construct, the hCTFbax mBS chimera, and the single-point mutants A1254T and V1258A in hCTFbax were stimulated with GAP10 or GAP10-Pro1 upon stable expression in HEK293 cells. Activation was measured in calcium transient assays, in $n = 2$ technical replicates. Data, expressed as mean \pm SD, represent $n = 4$ independent experiments, with $n = 2$ –4 technical replicates per group. See **Supplementary file 2** for potency and statistical details. **(C)** Calcium transients evoked in HEK293 cells stably expressing hCTFbax or the mutated construct G1011K upon stimulation with GAP10 or GAP10-Pro1. Data represent $n = 4$ independent experiments, with $n = 3$ technical replicates per group. Data are expressed as mean \pm SD. See **Supplementary file 2** for potency and statistical details.

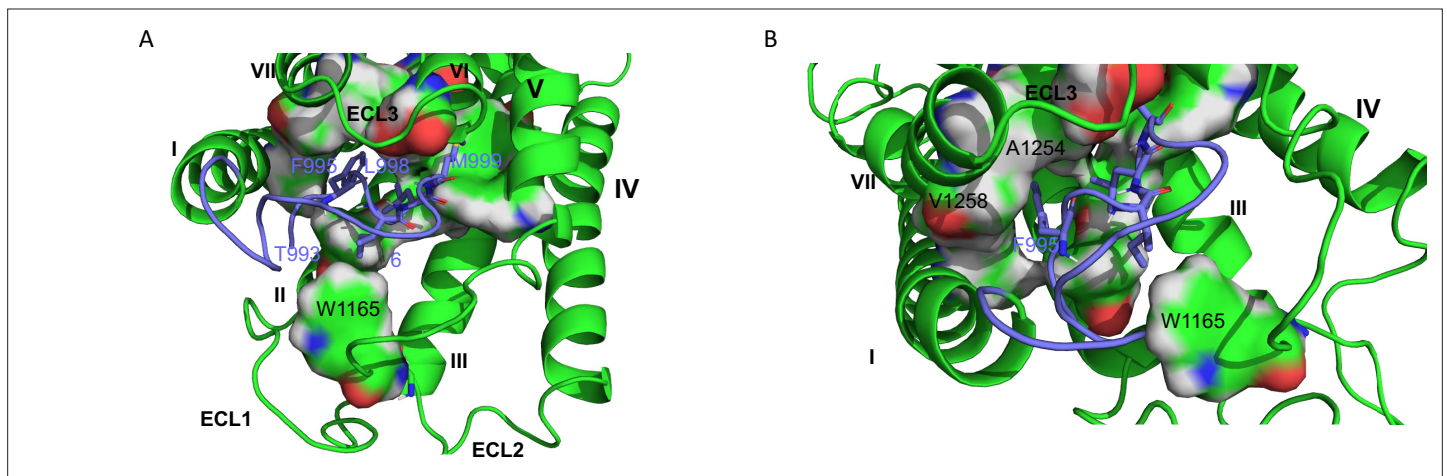


Figure 8. hGPR116 7TM homology model. **(A)** Binding model of the tethered agonist peptide (T993-L1010, C atoms in purple) to the transmembrane domain of human GPR116 homology model (C atoms in green). For clarity, only the four amino acids of the tethered agonist peptide that form most of the interactions with the transmembrane domain of GPR116 are displayed as sticks (F995, I997, L977, and M999). The amino acids of GPR116 transmembrane domain that interact with the four amino acids of the tethered agonist peptide mentioned above are displayed as surface color-coded by atom type (C in green, H in gray, N in blue, and O in red). **(B)** Zoom on A1254 and V1258, which form van der Waals contacts with F995.